International Journal of Ecology and Environmental Sciences 44 (3): 239-250, 2018
ISSN: 2320-5199 (Online)

Mesoscale Eddies and Yellowfin Tuna Catches in the Western Arabian Sea

SERGEY A. PIONTKOVSKI [1]*AND KHALID A. AL-HASHMI [2]

College of Agricultural and Marine Sciences, Sultan Qaboos University, P.O. Box 34, Al-Khod 123, Sultanate of Oman
E-mail ID: [1] spiontkovski@gmail.com; [2] khalidmat@gmail.com
* Corresponding author.

ABSTRACT

Daily maps of sea surface heights retrieved with 4-km spatial resolution from the MODIS-Aqua scanner and obtained over 13 years of remote sensing (from 2002 to 2015) were used to quantify monthly variations of 1108 cyclonic and 1090 anti-cyclonic eddies. The seasonal cycle of eddy occurrence has demonstrated two peaks, both corresponding to the spring and fall Inter-monsoon seasons. The amount of eddies observed during Inter-monsoon seasons was by ~ 30% higher than those of the South-west (winter) and North-east (summer) monsoons. Seasonal cycles of eddy occurrence were compared to Yellowfin Tuna landings. Two peaks of landings corresponding to April and October (which are cores of the spring and fall Inter-monsoon seasons) were observed. A positive linear correlation between the total number of cyclonic plus anti-cyclonic eddies and Yellowfin Tuna landings was statistically significant. Also, it holds for the cyclonic and anticyclonic eddies analyzed separately. Results of the Principal Component Analysis incorporating 12 environmental parameters (including wind speed, sea surface temperature, dissolved oxygen, nutrients, chlorophyll-a, sardine catches, and key indices of atmospheric anomalies) demonstrated that mesoscale eddies might be treated as ecologically important regional phenomena affecting seasonal variations of Yellowfin Tuna landings over the Omani shelf.

Key Words: Arabian Sea; Mesoscale Eddies; Yellowfin Tuna

INTRODUCTION

Eddies in the ocean have been reported over multiple spatial scales ranging from one hundred thousand kilometers (which is the scale of subtropical oceanic gyres) to the microscale resembling turbulent diffusion processes (Man and Lazier 2006). Mesoscale eddies with a typical size of 100-200km and the life span from several weeks to months, are common elements of the World Ocean physical dynamics. A number of reviews have synthesized tracks, occurrence, and mechanisms generating these eddies (Chelton et al. 2007, 2011)as well as their role in the transport of heat, salt, and energy (Chaigneau et al. 2011; L'Hégaret et al. 2013). Differences in eddy rotation and their kinetic energy impose a profound effect on biological processes. In the northern hemisphere, cyclonic eddies, with an anti-clockwise rotation induce the upward transport of a water mass from the depth to the surface, which enriches the euphotic layer with nutrients favoring high primary production. The process is opposite in anti-cyclonic eddies rotating clockwise. High packed fields of cyclonic and anticyclonic eddies result in a marked spatial-temporal variation of nutrients and primary productivity in the upper layer of the ocean (Piontkovski and Banse 2006)and feeding habitats for higher trophic levels (GodØ et al. 2012). In the north-west Atlantic, for instance, the longline fishery catches of bluefin tuna (*Thunnus thynnus*), were higher in the anticyclonic eddies than in the cyclonic ones, which was not the case for some other large pelagic predators (Hsu et al. 2015).

Mesoscale eddies of the western Arabian Sea have drawn much ofthe attention of marine biologists due to propagation through the region with intensive seasonal fluctuations of primary productivity driven by a powerful upwelling developed along the Omani shelf. Seasonal periodicity of upwelling (mediated by monsoonal winds) is footprinted in the thermo-haline haracteristics, distribution of dissolved oxygen concentration, nutrients, primary productivity, and small pelagic fish catches Marra and Barber 2005,Piontkovski and Jufaili 2013, Piontkovski and Al-Oufi2014, Wiggert et al. 2005). Much less attention was devoted to how eddies affect the upper trophic level of the pelagic ecosystem, in particularly large pelagic fishes. For instance, the artisanal fishery of Yellowfin Tuna in the Indian Ocean contributes about 30% of the total catch of various countries (Herrera et al. 2012) and dominates artisanal fishery over the Omani shelf (Fishery Statistics Book 2012, 2015).

Our study aimed at elucidating the seasonal cycle of cyclonic and anti-cyclonic eddy occurrence. We hypothesized that if it exists;this cycleshould influence the seasonality of landings of Yellowfin Tuna (*Thunnus albacares*).

MATERIALS AND METHODS

156 daily images of sea surface heights (retrieved with 4-km spatial resolution from MODIS-Aqua) were used, to estimatethe daily amounts of cyclonic and anticyclonic eddies for the western Arabian Sea (10-23ºN, 45-65ºE), for the 13 year period, from2002 to 2015. Maps were acquired from the CCAR Global Near Real-Time SSH Anomaly/Ocean Color Data Viewer (https://eddy.colorado.edu//ccar/data_viewer/index).In following general elements of the approach used by Cheltonet al. (2007, 2011) and Arur et al. (2014), the outermost closed contour resembling a vortex with minimum 5 cm amplitude, was identified as an eddy. Cyclonic eddies (with anticlockwise rotation) were characterized by negative sea surface height anomalies depressed in cores of eddies, while anti-cyclonic eddies (with clockwise rotation) have positive sea surface height anomalies elevated in cores, within the bounding contour.

In order to analyze spatial-temporal patterns of regional circulation with a special reference to mesoscale eddies, the HYCOM model hindcasts were used. This model performs an application of eddy-resolving basin-scale ocean hindcast, nowcast and forecast systems with high vertical discretization and the capability to apply additional coordinate surfaces to the mixed layer (Chassignet et al. 2007). This allows vertical mixing turbulence to be resembled. In being isopycnal in the open stratified ocean, the model reverts to a terrain-following coordinate in shallow coastal regions, and to z-level coordinates near the surface in the mixed layer. For the western Arabian Sea, the 32 vertical layer model was employed, at the resolution of 7 km.

Historical data on CTD casts were taken from the reports of the "Mustaquila 1" voyages along the Omani shelf, in 2007-2008 (McKoy et al. 2009). Conductivity, temperature, density, depth, and dissolved oxygen concentration were measured using an RBR CTD probe deployed from the vessel. The other data set used to estimate spatial heterogeneity of the dissolved oxygen concentration in the region was the 30th voyage of the R/V "Professor Vodyantisky", which carried out CTD casts in February-March, 1990 (Piontkovski and Banse 2006).

Data on Yellowfin Tuna landings using a sampling system established by the Oman-American USAID project (Mathews et al. 2011) have been regularly collected by the Department of Fisheries Statistics. Landings were recorded by categories entitled in archived materials as "Large Pelagics", "Small Pelagics", "Demersal", "Unidentified Fishes", and etc. Within these categories, fish is distributed over taxonomic groups. These data are available from the annual reports published by the Ministry of Agriculture and Fisheries (Fishery Statistics Book 2012, 2015).

The "Statistica" v.9 software was used for the regression analysis, as well as for the plots featuring a seasonal pattern of Yellowfin Tuna landings.

In assembling data for the Principal Component Analysis (PCA), 12 environmental parameters were retrieved, namely the sea surface temperature, zonal component of the wind speed, meridional component of the wind speed, concentration of dissolved nitrates, concentration of chlorophyll-a, the Indian Ocean Dipole index (IOD), the North Atlantic Oscillation index (NAO), the Multivariate El-Ninõ South Oscillation index (MEI), sardine catches (treated as the indicator of food source for tuna), YellowfinTuna catches, frequency of occurrence of cyclonic and anticyclonic eddies. For the assessment of factor loadings, the Varimax normalized matrix was applied to these environmental variables. The Principal Component Analysis was constrained by the extraction of two factors (principal components), which could explain the major part of the total variance in the system of selected variables.

RESULTS

The Oman Coastal Current (which is a synonym of the East Arabian Current) is the main component of regional circulation. This current is an extension of the Somali Current and is driven by the Southwest monsoon and flows north-east along the Omani coast, with a velocity of 0.5-0.8 m s^{-1} (Figure 1). During the South-west Monsoon, the confluence of the Oman Coastal Current and the outflowing Sea of Oman current forms a frontal zone near the most eastward land projection of Oman, named Ras Al Hadd. The water mass transport induced by this confluence ranges from 2 to 8 10^6 m^3 s^{-1} (Böhm et al. 1999). The other phenomenon induced by the confluence is a dipolar system consisting of acyclonic and anticyclonic eddies formed on front sides.

In analyzing the vertical structure of the Oman Coastal Current, one could see warmhighly aerated salty water occupying the upper mixed layer. High salinity is formed by the excess of evaporation over precipitation, as well as high saline waters coming from the Arabian (Persian) Gulf and the Gulf of Aden. A sharp interface with colder and fresher Arabian Sea water (at about 35m deep) is another characteristic feature of the thermohaline structure (Figure 1). The increase of salinity and density at 200-250m denotes the location of the Persian Gulf Water Mass. The dissolved oxygen concentration diminishes markedly, from 5 mL L^{-1} in the upper mixed layer, down to 1 mL L^{-1} observed at 70 m. The vertical profiles presented, exemplify the water mass structure at the edge of the Omani shelf.

As far as the open waters of the western Arabian Sea are concerned, data of the R/V "Professor Vodyanitsky" were analyzed (Figure 2). The uniqueness of these data is contributed by direct CTD casts (with oxygen sensor) carried out in the form of regular grid of 142 oceanographic stations which covered a huge area and resembled the mesoscale variability from the surface to 1000 m. Eddies with the diameter of ~100 km were the main components inducing spatial heterogeneity of the oxygen field and the other CTD parameters. For instance, the mean oxygen concentration (sampled over 86 stations at 100m) was equal to 2 mL L^{-1}, and exhibited the variation coefficient of 49%.

A current setup of the HYCOM model resembled the whole Arabian Sea basin (Figure 3, upper panel), which in fact was bigger than the area we used, to assess the seasonality of eddy occurrence. As far as the western part of the Arabian Sea is concerned,maps of geostrophic currents (lined up seasonally) implied three typical episodes of regional circulation. For instance, in July, the Oman Coastal Current was well pronounced and a general water mass transport was directed to the north-east. The fall Inter-monsoon season (exemplified by the month of October) showed no clearly directed geostrophic flow. However, several mesoscale eddies were well contoured, along the Omani shelf. In February, during the North-east Monsoon, the Oman Coastal Current is reversed to the south-west. These episodes implied the speed of the geostrophic current tovary seasonally, in the range from 5 to 90 cm s^{-1}.

The model maps have elucidated a number of eddies persisting throughout the annual cycle. In order to acquire the seasonal occurrence of eddies more accurately; a direct(remotely sensed) sea surface altimetry was used. Daily maps of remotely sensed sea surface heights exemplified the eddy field in the form of two fragments featuring the South-west monsoon and spring Inter-monsoon seasons (Figure 3, midpanel). One could see well pronounced cyclonic and anticyclonic eddies, occupying the western Arabian Sea, including the Omani shelf. The interaction of cyclonic and anti-cyclonic eddies forms frontal zones with sharp gradients of physical and chemical parameters. For instance, for the episode in Figure 3 (low panel), a spatial gradient of the sea surface temperature in regions of interacting eddies consisted of~0.1°C km^{-1}.

Daily maps of sea surface heights obtained over 13 years (2002-2015) were used to quantify monthly variations of 1108 cyclonic and 1090 anti-cyclonic eddies in the region (Figure 4). Positive and negative sea surface height anomalies matching the range of 10-20 cm were the most numerous. The seasonal cycle of monthly eddy occurrence has demonstrated two peaks both corresponding to the spring and fall Inter-monsoon seasons. Magnitudes of both peaks have the same level pointing at a fairly stable number of eddies persisting during inter-monsoon seasons. The amount of eddies observed during inter-monsoon seasons was by ~ 30% higherthan those of the South-west (winter) and North-east (summer) monsoons. Seasonal cycles of occurrence of cyclonic and anti-cyclonic eddies were fairly similar ($r= 0.6$, $p= 0.03$).

Seasonal cycles of eddy occurrence were compared to Yellowfin Tuna landings. Two peaks of landings corresponding to April and October (which are cores of spring and fall inter-monsoon seasons) were observed (Figure 5). The correlation between the total number of cyclonic plus anti-cyclonic eddies and Yellowfin Tuna landings was statistically significant (Figure 6; $r= 0.6$; $p= 0.04$). Also, it holds for the cyclonic and anticyclonic eddies, analyzed separately.

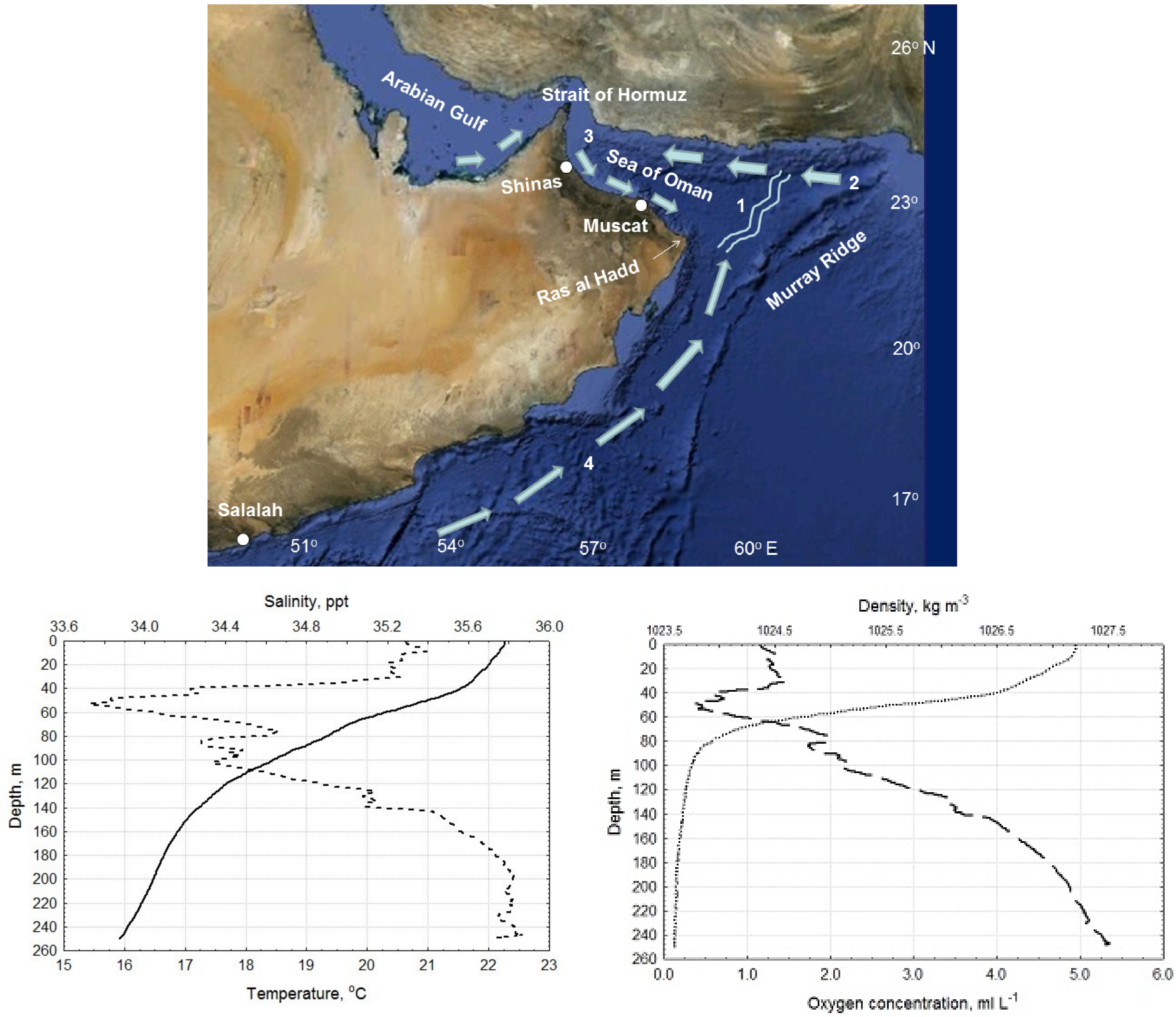

Figure 1. The system of currents and fragments of the vertical structure.
Upper panel: Background image: three-dimensional bathymetric map (www.earth.google.com). Two parallel lines (1) demarcate the location of the Ras Al Hadd frontal zone formed by the confluence of currents (3 and 4). Arrows (2-4) indicate direction of the main currents (in summer through fall period). (2): inflow of the Indian Ocean Water mass, (3): outflow of the (Arabian Gulf) Persian Gulf Water mass, and (4): Oman Coastal Current (East Arabian Current). Lower panel: The vertical structure of the Oman Coastal Current (August 2008, 18°19.8N, 57°33.4E).

To estimate the role of the other environmental characteristics potentially affecting Yellowfin Tuna landings, data on 12 parameters were seasonally averaged for the region and subjected to the Principal Component Analysis (Figure 7). In assembling data covering 13 years of monthly measurements, a number of data sources were used. Data on the concentration of dissolved oxygen and nitrates were retrieved from the SQU database on coastal monitoring. The remotely sensed chlorophyll-a time series from 2002 to 2014 were downloaded from the MODIS scanner website (http://oceancolor.gsfc.nasa.gov). Time series on SST, wind speed, MEI, NAO and IOD atmospheric indices were downloaded from the NCAR/NCEP database- http://www.esrl.noaa.gov/psd/data[20].

It seemed important to employ the global scale atmospheric anomalies (like MEI and NAO) having a profound effect on the western Arabian Sea, as well as

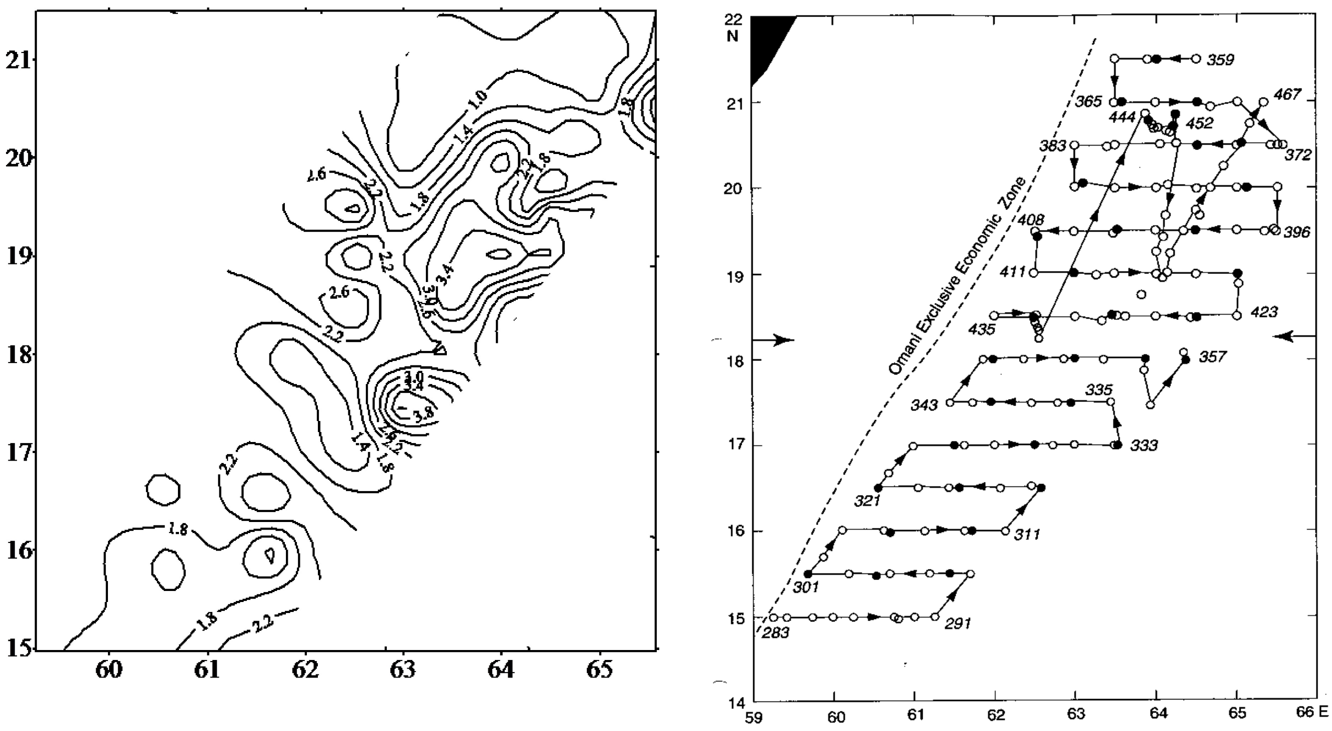

Figure 2. Spatial heterogeneity of the dissolved oxygen concentration (R/V "Professor Vodyanitsky, February –March, 1990; Piontkovski and Banse, 2006). Upper panel: Spatial distribution of the dissolved oxygen concentration (ml L^{-1}, at 100 m). Lower panel: Spatial grid of oceanographic stations used to sample the dissolved oxygen concentration.

the regional ones, represented by the Indian Ocean Dipole (IOD). The MEI index represents the first unrotated principal component of atmospheric variables measured over the tropical Pacific. Negative values of the MEI stand for the cold El-Niňo Southern Oscillation (ENSO)while positive values stand for the warm El-Niňo phase (Wolter and Timlin 1993). Footprints of the North Atlantic Oscillation (NAO) and ENSO atmospheric anomalies were reported for physical dynamics of the Arabian Sea (Cullen et al. 2002, Kahya 2011, Reason et al. 2000). A regional IOD is characterized by anomalously cold sea surface temperatures in the south eastern part of the Equatorial Indian Ocean versus the anomalously warmed south-western part. Fluctuations of sea surface temperature during IOD are driven by changes to the wind field of the central equatorial Indian Ocean. In response to anomalies of the wind field, the thermocline rises in the eastern and deepens in the western parts of the ocean.

The essence of the PCA is the data compression enabling the number of variables used to describe the variability of data to be reduced to a few Principal Components (Factors). A statistical procedureof such a reduction is based on a rotation of the coordinate system of variables. In the new coordinate system,they all are uncorrelated.The extraction of eigenvectors of the matrix enables one to reduce the diversity of numerous variables to a few Principal Components (Factors) in which the component scores are standardized units based on a correlation matrix. In fact, the eigenvectors are the results of the projection of the original variable axes into the space of new Principal Components. Eigenvectors forming the principal components are based on the similarity coefficients in linear combinations of variables. Once the internal structure of Principal Components is elucidated and these components are interpreted (labeled) in some way, the relationship between the first two leading components might be analyzed in the form of a scatterplot (Figure 7).

The First Principal Component was contributed mainly by atmospheric characteristics (namely MEI, NAO, zonal and meridional components of the wind speed). Their load was complemented by SST and concentration of dissolved nitrates. A statistical load of

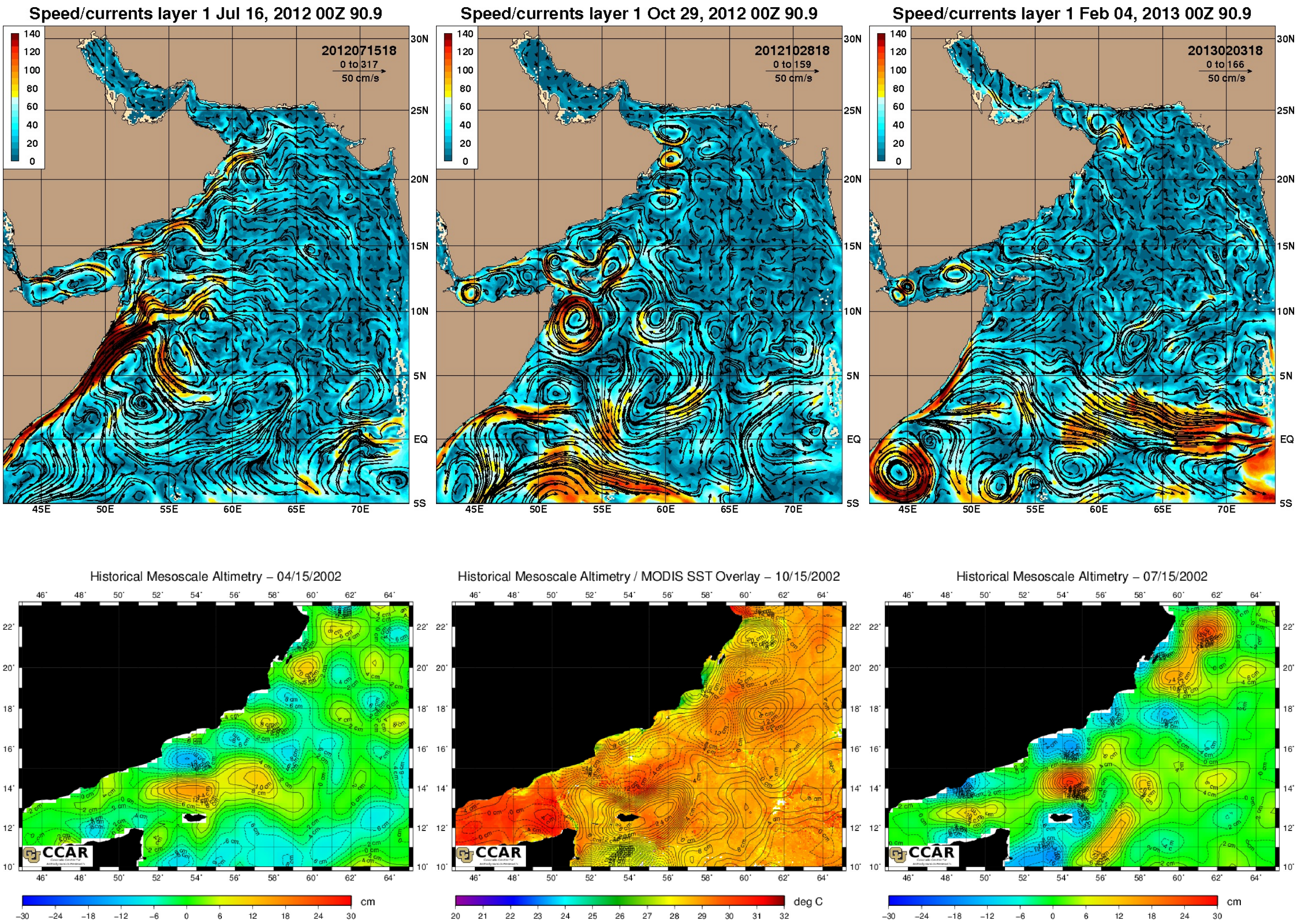

Figure 3. Seasonal circulation in the western Arabian Sea. Upper panel: fragments of geostrophic currents over seasons retrieved from the HYCOM model. Mid panel: examples of sea surface height anomalies resembling mesoscale eddies observed along the Omani shelf during Spring Inter-monsoon and the Southwest Monsoon periods, in 2002. Color scale stands for sea surface height anomalies (cm). Lower panel: color scale stands for the sea surface temperature (°C) superimposed on sea surface height anomalies given by contour lines (cm).

the Second Principal Component was contributed by Yellowfin Tuna catches, frequency of occurrence of cyclonic and anticyclonic eddies and the concentration of the dissolved oxygen. All in all, both principal components have "explained" 66% of the total variance of the constructed system of variables.

DISCUSSION

In fact, a biannual seasonal cycle of eddy occurrence (with peaks corresponding to Inter-monsoon seasons) stands in line with many other seasonal processes in physical dynamics of the western Arabian Sea. The data we obtained over 13 years modify our previous findings based on the analysis period of one year (Piontkovski and Jufaili 2013).

The Oman Coastal Current (the East Arabian Current) is the major element of circulation in the western Arabian Sea (Kindle 2002, Shi et al. 2000). The maps exemplified in Figure 3 have pointed out that the flow is meandering. A part of eddies observed in the region is generated by the Omani Coastal Current which periodically interacts with bottom topography (L'Hégaret et al. 2013). Also, the current deteriorates during inter-monsoon periods, which generates additional eddies and influences the seasonality of their occurrence. Moreover, the animation of weekly images of sea surface heights we constructed (but could not display here), clearly pointedto a propagation of eddies

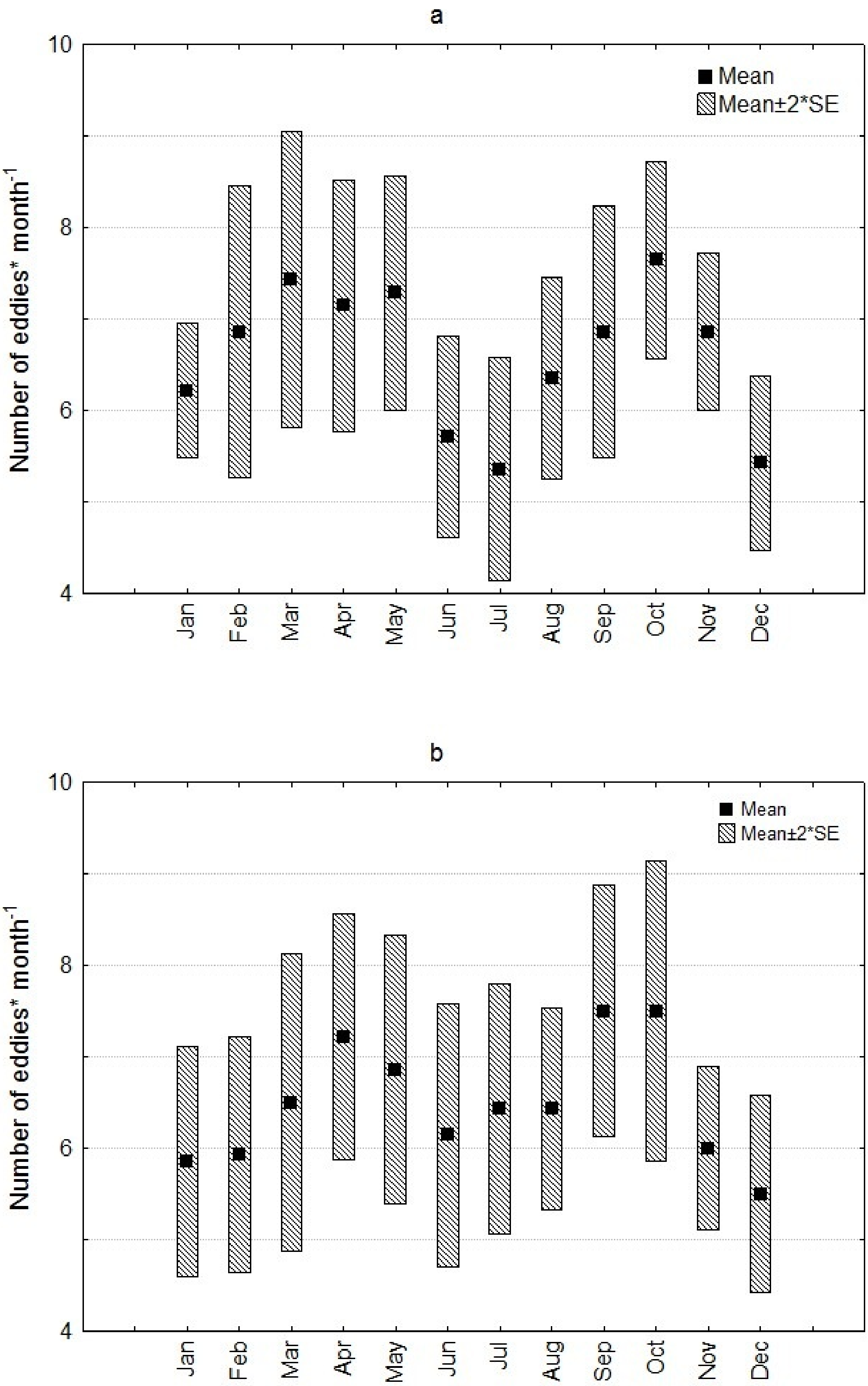

Figure 4. Seasonal changes of (a) cyclonic and (b) anti-cyclonic eddy occurrence in the western Arabian Sea.

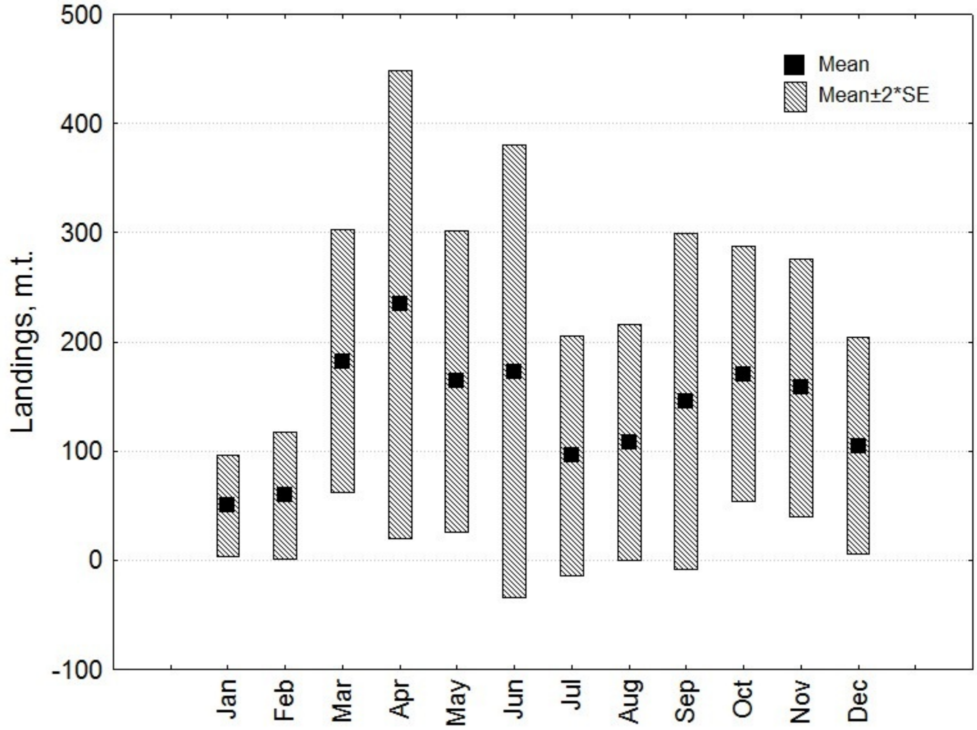

Figure 5. Seasonal changes of artisanal landings of Yellowfin Tuna over the Omani shelf.

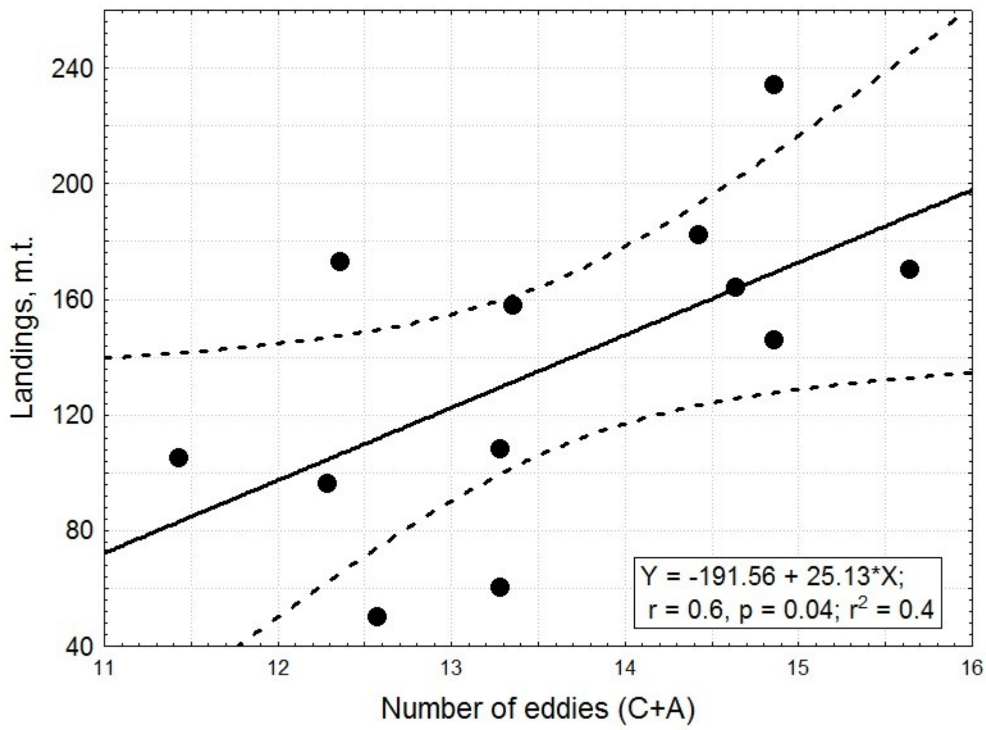

Figure 6. Relationship between eddy occurrence and Yellowfin Tuna landings over the Omani shelf. C: cyclonic eddies. A: anti-cyclonic eddies.

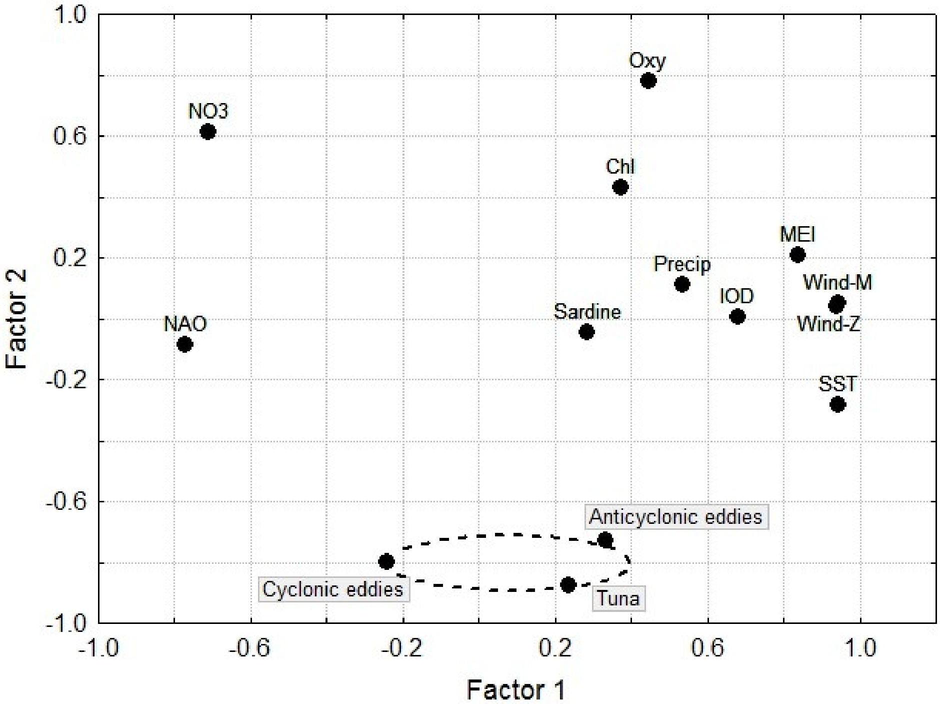

Figure 7. Factor loading: the eigen value extraction by the Principal Component Analysis.
NAO: North Atlantic Oscillation index, NO_3: concentration of dissolved nitrates, Oxy: concentration of dissolved oxygen, Chl: concentration of chlorop.yll-a, MEI: Multivariate El-Ninõ South Oscillation index, IOD: Indian Ocean Dipole index, Precip: Atmospheric precipitation, Win-M and Wind-Z: Meridional and zonal components of wind speed, Sardine: sardine catches, Tuna: Yellowfin Tuna catches.

from the Arabian Sea interior towards the Omani shelf. These eddies are believed to be formed by baroclinic Rossby waves which are known to travel westward (Chelton et al. 2007, McCreary et al. 1993, Subrahmanyam and Robinson 2000). At the equator, for instance, these waves propagate at a speed of 13 km d^{-1}, which decreases from the equator to the north (Jensen et al. 2014).

Standard deviations on plots featuring the seasonality of eddy occurrenceimplied high variance of the seasonal cycle, which is presumably associated with a broad range of years averaged in our plots (2002-2015). Indeed, a breakdown of seasonal cycles pointed out marked shifts of peaks over months, as well as marked variability of magnitudes of eddy occurrence over years (Figure 8). For example, the year 2007 (which exhibited the lowest frequency of eddy occurrence) was the year of high atmospheric anomalies accompanied by powerful hurricane "Gonu" affecting the western Arabian Sea and resulted in a landfall on the Omani coast in June. On the other hand, maximal frequency of eddy occurrence was observed in 2015 which was the most powerful El-Ninõ year since 1997. The eddy activity is known to be maximal during El-Ninõ years (Chaigneau et al. 2008). One of the possible mechanisms is that El-Ninõ events destabilize the current through enhancement of the velocity shear in the vertical, which results in the formation of eddies (Melsom et al. 1999). These examples point out that inter-annual variability induced a notorious "noise" in assessments of seasonal trends of eddy occurrence in the region.

Interestingly, the ratio of cyclonic to anticyclonic eddies was fairly stable over seasons. This points to an equal number of cyclonic to anticyclonic eddies observed in the western Arabian Sea throughout the annual cycle. The same ratio of cyclonic to anti-cyclonic eddies was reported for the South Indian Ocean, for eddies with radius ≥100km (Zheng et al. 2015).

A vulnerability of large pelagic (including tuna) species to mesoscale eddies and frontal zones generated by these eddies was observed for the number of regions (Laurs et al. 1984, Solanki et al. 2005, 2008). For example, the Atlantic Bluefin tuna catch per unit of efforts was significantly higher in areas with negative sea surface height anomalies and cooler sea surface temperatures, which were characteristic of mesoscale cyclonic eddies in the Gulf of Mexico (Teo and Block

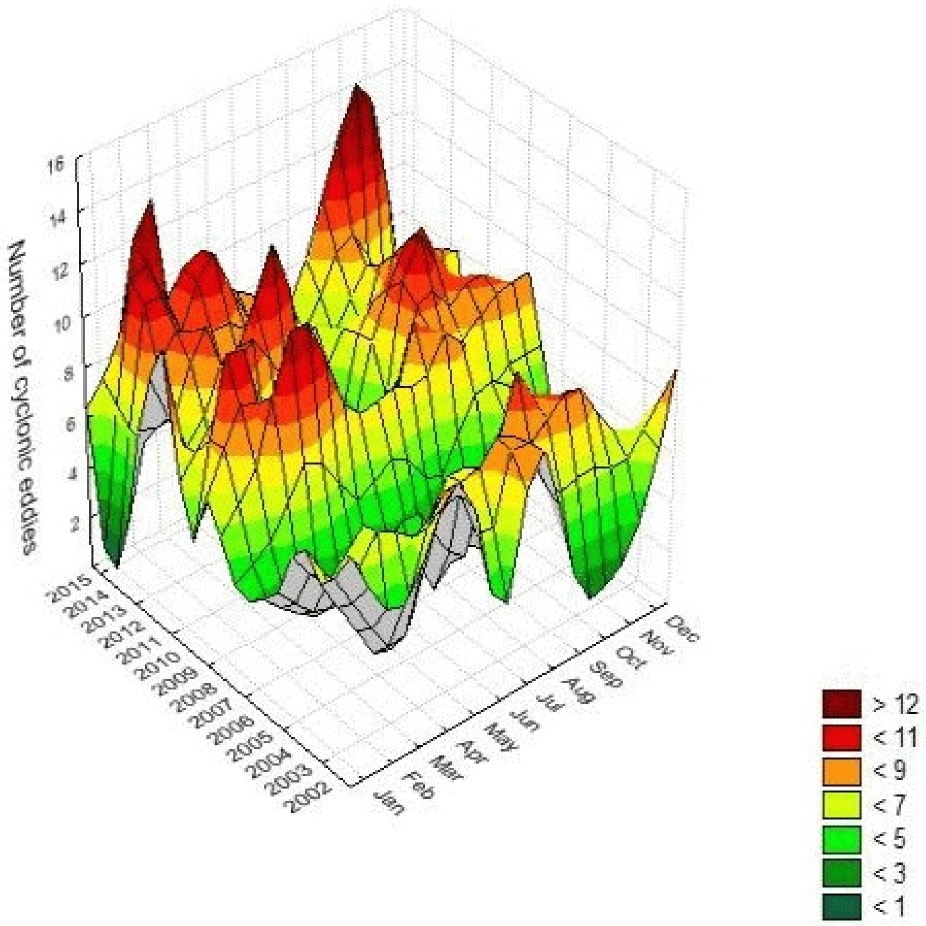

Figure 8. The frequency of occurrence of cyclonic eddies: inter-annual variation of seasonal cycles.

2010). As far as a preferential range of temperatures is concerned, Yellowfin Tuna prefers warm waters with temperatures above 25ºC (Lan et al. 2012a). In terms of vertical stratification of habitats, tuna schools are sensible to a shoaling of the thermocline-the phenomenon which could periodically increase tuna catches (Lan et al. 2012b). In the eastern Indian Ocean, the mean catch of large and small pelagic fish per unit of efforts was observed to vary significantly ($p<0.001$) among the different eddy zones, thus showing a strong link between the eddy activity and performance of fishery (Arur et al. 2014).The relationship we elucidated between the seasonality of eddy occurrence and tuna landings is consistent with these reports.

Large pelagic predators are active swimmers sensible to low concentrations of the dissolved oxygen due to their high metabolism. The concentration less than 3.5 ml L^{-1} induces symptoms of stress for many tropical pelagic fishes; therefore, this concentration is interpreted as the hypoxic threshold (Prince and Goodyear 2006, Stramma et al. 2012). Therefore, tropical tuna species usually remain shallower than 100 m (Matsumoto et al. 2016). In the upper 100m layer of the western Arabian Sea, cyclonic eddies shift the seasonal oxycline upwards and induce spatial heterogeneity in the distribution of the oxygen concentrations which could be, regionally, below this threshold. The map of dissolved oxygen concentration based on direct sampling carried out in the form of regular grid of oceanographic stations has exemplified“patches”of low oxygen concentration associated with eddy location (Figure 2). Presumably, these eddies impact the spatial distribution of Yellowfin Tuna and might be treated as constituents of the mechanism mediating the relationship between the frequency of eddy occurrence and magnitudes of tuna landings. Our simple estimates point out that couple of cyclonic eddies (with a diameter of ~100 km) passing through relatively narrow Omani shelf would cover about 50% of its area.

So the potential impact of eddies should be huge taking into account that the main part of tuna landing comes from shelf waters.

CONCLUSION

Pilot results of the PCA and regression analyseshave demonstrated thatmesoscale cyclonic and anticyclonic eddies might be treated as ecologically important regional phenomena affecting seasonal variations of Yellowfin Tuna landings over the Omani shelf.

ACKNOWLEDGMENTS

We would like to thank Muna Al-Tarshi, Sabrina Al-Ismaili, Sultana Al-Jardani, and Yasmin Al-Alawi for assistance with quantifying eddy frequency. This research was funded by the SQU grant # IG/AGR/FISH/17/01.

REFERENCES

Arur, A.; Krishmam, P.; George, G.; Bharathi, M.P.G.; Kaliya-moorthy, M.; Shaeb, K.H.B.; Suryavanshi, A.S.; Kumar, T.S. and Joshi A.K. 2014.The influence of mesoscale eddies on commercial fishery in the coastal waters of the Andaman and Nicobar Islands, India. International Journal of Remote Sensing 35: 6418-6443.

Böhm, E.; Morrison, J.M.; Manghnani, V.; Kim, H.S. and Flagg, C.N. 1999. The Ras al Hadd Jet: remotely sensed and acoustic Doppler current profiler observations in 1994-1995. Deep-Sea Research II, 46: 1531-1549.

Chaigneau, A.; Gizolme, A. and Grados, C. 2008. Mesoscale eddies off Peru in altimeter records: identification algorithms and eddy spatio-temporal patterns. Progress in Oceanography 79: 106-119.

Chaigneau, A.; Le Texier, M.; Eldin, G.; Grados, C. and Pizarro, O. 2011. Vertical structure of mesoscale eddies in the eastern South Pacific Ocean: A composite analysis from altimetry and Argo profiling floats. Journal of Geophysical Research 116, C11025, doi:10.1029/2011JC007134

Chassignet, E.P.; Hurlburt, H.E.; Smedstad, O.M.; Halliwell, G.R.; Hogan, P.J.; Wallcraft, A.J.; Baraille, R. and Bleck, R. 2007. The HYCOM (Hybrid Coordinate Ocean Model) data assimilative system. Journal of Marine Systems 65: 60-83.

Chelton, D.; Schlax, M.G.; Samelson, R.M. and de Szoeke, R.A. 2007. Global observations of large oceanic eddinies. Geophysical Research Letters 34, L15606: doi:10.1029/2007GL030812

Chelton, D.B.; Schlax, M.G. and Samelson, R.M. 2011. Global observations of nonlinear mesoscale eddies. Progress in Oceanography 91: 167-216.

Cullen, H.M.; Kaplan, A.; Arkin, P.A. and de Menocal, P.B. 2002. Impact of the North Atlantic Oscillation on Middle Eastern climate and stream flow. Climate Change 55: 315-338.

Fishery Statistics Book. 2012. Fisheries Statistics and Information Department. General Directorate of Fisheries Research. Ministry of Agriculture and Fisheries. Sultanate of Oman. Muscat. 237 pages.

Fisheries Statistics Book. 2015. Ministry of Agriculture and Fisheries. Sultanate of Oman. Muscat. 163 pages.

Godø, O.R.; Samuelsen, A.; Macaulay, G.; Patel, R.; Hjøllo, S.S.; Horne, J.; Kaartvedt, S. and Johannessen, A. 2012. Mesoscale eddies are oases for higher trophic marine life. PLoS ONE 7, 330161, doi: 10.1371/journal.pone.0030161

Herrera, M.; Pierre, L.; Geehan, J. and Milion, J. 2012. Review of the statistical data and fishery trends for tropical tunas. Indian Ocean Tuna Commission, IOTC-2012-WTTT14-07 Rev 1: 1-62

Hsu, A.; Boustany, C.; Roberts, A.M.; Chang, J.H. and Halpin, P.N. 2015. Tuna and swordfish catch in the U.S. northwest Atlantic longline fishery in relation to mesoscale eddies. Fisheries Oceanography 24: 508–520.doi: 10.1111/fog.12125

Jensen, V.E.; Samuel, P. and Johannessen, O.M. 2014. Mesoscale studies in the Indian Ocean using altimeter data. ESA Earthnet Online. European Space Agency, https://earth.esa.int/workshops/ers97/papers/jensen/jensen-et-al.html. Accessed 08/05/2016.

Kahya, E. 2011.The impacts of NAO on the hydrology of the Eastern Mediterranean. Advances in Global Change Research 46: 57-71.

Kistler, R.; Kalnay, F.; Collins, W.; Saha, S.; White, G.; Woollen, J.; Chelliah, M.; Dool, W.; Jenne, R. and Fiorino, M.2001. The NCEP-NCAR 50-Year Re-analysis: Monthly Means CD-ROM and Documentation. Bulletin of the American Meteorological Society 82: 247-268.

Lan, K.W.; Nishida, T.; Lee, M.A.; Lu, H.J.; Huang, H.W.; Chang, S.K. and Lan, Y.C. 2012a.Influence of the marine environment variability on the Yellowfin tuna (*Thunnusalbacares*) catch rate by the Taiwanese longline fishery in the Arabian Sea, with special reference to the high catch in 2004. Journal of Marine Science and Technology 20: 514-524.

Lan, K.W.; Lee, M.A.; Nishida, T.; Lu, H.J.; Weng, J.S. and Chang, Y. 2012b. Environmental effects on Yellowfin tuna catch by the Taiwan longline fishery in the Arabian Sea". International Journal of Remote Sensing 33: 7491-7506.

L'Hégaret P.; Lacour L.; Carton X.; Roullet G.; Baraille R. and Corréard S. 2013.A seasonal dipolar eddy near Ras Al Hamra (Sea of Oman).Ocean Dyn 63: 633-659

Laurs, R.M.; Fiedler, P.C. and Montegomery, M. 1984. Albacore catch distributions relative to environmental features observed from satellite. Deep-Sea Research 31: 1085-1099.

Mann, K.H. and Lazier, J.R.N. 2006. Dynamics of Marine Eco-systems. Blackwell Publishing, Oxford. 496 pages.

Marra, J. and Barber, R.T. 2005. Primary productivity in the Arabian Sea: A synthesis of JGOFS data. Progress in Oceanography 65: 159–175.

Mathews, C.P.; Al-Mamry, J. and Al-Habsy, S. 2001. Precautionary management of Oman's demersal fishery. In: First International Conference on Fisheries, Aquaculture and Environment in the NW Indian Ocean. Sultan Qaboos University, Muscat.

Matsumoto, T.; Satoh, K.; Semba, Y. and Toyanga, M. 2016. Comparison of the behavior of skipjack (*Katsuwonus pelamis*), yellowfin (*Thunnus albacares*) and bigeye (*T. obesus*) tuna associated with drifting FADs in the equatorial central Pacific Ocean. Fisheries Oceanography 25: 565-581.

McCreary, J.P.; Kundu, P.K. and Molinari, R.L. 1993. A numerical investigation of dynamics, thermodynamics, and mixed layer processes in the Indian Ocean. Progress in Oceanography 31: 181-244.

McKoy, J.; Bagley, N.; Gauthier, S. and Devine, J. 2009.Fish Resources of the Arabian Sea coast of Oman: Project Summary. In: Technical Report 1. Bruce Shallard and Associates. Muscat

Melsom, A.; Meyers, S.D.; Hurlburt, H.E.; Metzger, J.E.; O'Brien, J.J. 1999. ENSO effects on Gulf of Alaska eddies. Earth Interactions 3: 1-30.

Piontkovski, S.A. and Banse, K. 2006. Overview of results. In: K. Banse, and S.A. Piontkovski, (Editors). The Mesoscale Structure of the Epipelagic Ecosystem of the Open Northern Arabian Sea. Universities Press, Hyderabad. 248 pages.

Piontkovski, S.A. and Al-Jufaili, S. 2013.Coastal upwellings and mesoscale eddies of the western Arabian Sea: some biological implications. International Journal of Oc Oceanography 7: 93-115

Piontkovski, S.A. and Al-Oufi, H.S. 2014.The oxygen minimum zone and fish landings along the Omani shelf. Journal of Fisheries and Aquatic Science 9: 294-310.

Prince, E.D. and Goodyear, C.P. 2006. Hypoxia-based compression of tropical pelagic fishes. Fish Oceanography 15: 451-464.

Reason, C.J.C.; Allan, R.J.; Lindesay, J.A. and Ansell, T.J. 2000. ENSO and climatic signals across the Indian Ocean basin in the global context. Part I. International Composite Patterns. International Journal of Climate 20: 1285-1327.

Shi, W.; Morrison, J.M.; Bohm, E. and Manghnani, V. 2000.The Oman upwelling zone during 1993, 1994 and 1995. Deep-Sea Research II, 47: 1227-1247.

Solanki, H.U.; Mankodi, P.C.; Nayak, S.R. and Somvanshi, V.S. 2005. Evaluation of remote-sensing-based potential fishing zones (PFZs) forecast methodology. Continental Shelf Research 25: 2163-2173.

Solanki, H.U.; Mankodi, P.C.; Dwivedi, M. and Nayak, S.R. 2008. Satellite observations of main oceanographic processes to identify ecological associations in the Northern Arabian Sea for fishery resources exploration. Hydrobiologia 612: 269-279.

Stramma, L.; Prince, E.D.; Schmidtko, S.; Jiangang L.; Hoolihan, J.P.; Visbeck, M.; Wallace, D.W.R.; Brandt, P. and Körtzinger, A. 2012. Expansion of oxygen minimum zones may reduce available habitat for tropical pelagic fishes. Nature Climate Change 2: 33-37.

Subrahmanyam, B. and Robinson, I. 2000. Sea surface height variability in the Indian Ocean from TOPEX/POSEIDON altimetry and model simulations. Marine Geodesy 23: 167-195.

Teo, S.L.H. and Block, B. 2010.Comparative influence of ocean conditions on yellowfin and Atlantic bluefin tuna catch from longlines in the Gulf of Mexico. PLOS One 5: e10756; doi:10.1371/journal.pone.0010756

Wiggert, J.D.; Hood, R.; Banse K. and and Kindle J. 2005. Monsoon driven biogeochemical processes in the Arabian Sea. Progress in Oceanography 65: 176–213.

Wolter, K. and Timlin, M.S. 1993. Monitoring ENSO in COADS with a seasonality adjusted principal component index. Proceedings of the 17th Climate Diagnostics Workshop, Norman, OK, NOAA/NMC/CAC, NSSL, Oklahoma Climate Survey, CIMMS and the School of Meteorology, University of Oklahoma, pp.52-57

Zheng, S.; Du, Y. and Cheng, X. 2015. Eddy characteristics in the South Indian Ocean as inferred from surface drifters. Ocean Science 11: 361-371.

Received 28 March 2018
Accepted 31 May 2018